Influence of Pressure-Gradient and Shear on Ballooning Stability in Stellarators

S.R.Hudson 1), C.C.Hegna 2), N.Nakajima 3), R.Torasso 4), A.S.Ware 5), J.G.Wohlbier 2)

1) Princeton Plasma Physics Laboratory, P.O. Box 451, Princeton NJ 08543, USA.
2) Dept. of Engineering Physics, University of Wisconsin, Madison WI 53706, USA.
3) National Institute for Fusion Science, Oroshi-cho 322-6, Toki 509-5292, Japan.
4) Courant Institute of Mathematical Sciences, New York University, NY 10012, USA.
5) Dept. of Physics and Astronomy, University of Montana, Missoula, MT, 59812, USA.

shudson@pppl.gov

Abstract. Pressure driven, ideal ballooning stability calculations are often used to predict the achievable plasma β in stellarator configurations. In this paper, the sensitivity of ballooning stability to plasmas profile variations is addressed. A simple, semi-analytic method for expressing the ballooning growth rate, for each field line, as a polynomial function of the variation in the pressure-gradient and the average magnetic shear from an original equilibrium has recently been introduced [*Phys. Plasmas*, 11(9):L53, 2004.]. This paper will apply the expression to various stellarator configurations and comment on the validity of various truncated forms of the polynomial expression.

1. Introduction.

An economically viable fusion reactor must sustain high-pressure, stable equilibria. It is often predicted that short wavelength, pressure-driven instabilities, ballooning modes, are the instabilities that limit the obtainable plasma stored energy. An important prediction from tokamak stability studies was the appearance of the second region of stability [1], where sufficiently high pressure-gradient stabilizes the ballooning mode. There is no guarantee that second stable regions exist for general three-dimensional equilibria. Quantitative calculations are required to determine whether second stability is possible for any given configuration. It has been shown that some stellarators do [2, 3, 4], and that some stellarators do not [5, 6], possess second stable regions. The question thus arises : what property of the configuration determines whether a second stability region will exist?

The 'brute-force' approach to investigate this question is to numerically compute an equilibrium and solve the ballooning eigenvalue equation. The pressure is then increased and the process repeated. This process is tedious, particularly so given that computing a three-dimensional equilibrium is a computationally intensive task, and this approach imparts little insight. Furthermore, this method cannot ascertain if, beyond a region of instability, there lies a second stable region.

A better approach, the method of profile variations, was introduced by Greene & Chance [1] for axisymmetric configurations. They considered variations in the pressure-gradient and average shear at a selected magnetic surface in the equilibrium. The pressure-gradient and average shear have a crucial impact on ballooning stability, as the presence of pressure-gradients in regions of unfavorable curvature is the cause of ballooning instability, while shear is the dominant stabilizing mechanism. The equilibrium itself is then adjusted to preserve force balance, and a family of semi-analytic neighboring equilibria is constructed.

For each such constructed neighboring equilibrium, the ballooning equation may be resolved numerically (exactly) and marginal stability diagrams constructed. Such diagrams are widely used to study tokamak stability, and the analysis has been extended to stellarator geometry [2, 7]. This method eliminates the need to re-compute the equilibrium, and illuminates the role of the local magnetic shear.

The mechanism for second stability was determined to be that pressure induced variations in the parallel current, $J_\parallel = \mathbf{J}\cdot\mathbf{B}/B^2$, cause variations in the local shear, which may strengthen the stabilizing force in regions of unfavorable curvature. This stabilizing force may, depending on the geometry, overwhelm the destabilizing effect. A related pressure-induced stabilization phenomenon that should be mentioned, is when increased pressure alters the geometry of the configuration [8, 9, 10]. While this mechanism can modify the stability properties, it is generally a smaller effect, as is verified by equilibrium reconstruction and stability analysis [4].

Recently, the method of profile variations has been extended using an additional eigenvalue perturbation analysis [11]. It was shown that it is not necessary to re-solve the ballooning equation for the semi-analytic, neighboring equilibria. Whether ballooning stability will improve or degrade as the pressure-gradient is increased can be inferred from information obtained directly from the original equilibrium. An analytic polynomial expression for the eigenvalue γ, with numerically computed coefficients, for how the ballooning eigenvalue depends on variations in the pressure-gradient, $\delta p'$, and average shear, $\delta\iota'$, was derived.

In Section 2, an outline of the derivation will be presented. Initially, the method of profile variations is used to construct families of neighboring magnetostatic equilibria [1, 7]. Subsequently, a perturbation approach is employed to estimate the effect these variations have on the ballooning eigenvalue [11]. Full details of the method have been presented in Ref.[11] and references therein. In Section 3, the predictions of the expression for a variety of stellarator configurations will be explored, and Section 4 will expand upon some of the conclusions presented in Ref.[11]. In Ref.[11] it was claimed that a second stable region will exist if $\partial^2\gamma/\partial p'^2 < 0$. Here we show that this criterion is valid only if the higher order terms can be neglected.

2. Method.

For a given configuration, the the ballooning eigenvalue equation, where $\gamma = -\omega^2$ is the eigenvalue and $\gamma > 0$ indicates instability, is written [7]

$$[\partial_\eta P \partial_\eta + Q - \gamma R]\xi = 0, \tag{1}$$

where the ballooning coefficients P, Q, R are $P = B^2/g^{\psi\psi} + g^{\psi\psi}L^2, Q = 2p'\sqrt{g}(G + \iota I)(\kappa_n + \kappa_g L)$ and $R = \sqrt{g}^2 P$. Here L is the integrated local shear $L = \int_{\eta_k}^{\eta} s(\eta')d\eta'$ where $s = \iota' + \tilde{s}$ is the local shear (where $\tilde{s}$ denotes the part of the local shear that varies within a flux surface), and κ_n, κ_g represent the normal and geodesic curvatures. The normalized radial wavenumber, sometimes called the ballooning angle, $\eta_k\eta_k$, is that point chosen where the integrated local shear vanishes. This expression is written in Boozer coordinates [12] (ψ, θ, ζ) with the Jacobian $\sqrt{g} = (G + \iota I)/B^2$, and η is a parameter that measures distance along a field line. The eigenvalue γ is a function of the magnetic flux surface, ψ, magnetic field line label and η_k. Instability is a balance between the destabilizing pressure/curvature drive and the stabilizing effect of the local shear that

appears through L. This is an eigenvalue equation and for realistic geometry must be solved numerically. This paper will assume that the equilibrium is supplied numerically, and that the ballooning eigenvalue and eigenfunction (γ, ξ), for a given field line and given η_k, has been solved.

A family of semi-analytic, nearby equilibria may be constructed using the method of profile variations [1]. Variations in the pressure $p(\psi)$ and rotational-transform profiles $\iota(\psi)$ are introduced in the form

$$p(\psi) \rightarrow p(\psi) + \mu\, \delta p(y), \tag{2}$$
$$\iota(\psi) \rightarrow \iota(\psi) + \mu\, \delta\, \iota(y), \tag{3}$$

where μ is a small expansion parameter. The auxiliary variable $y = (\psi - \psi_b)/\mu$ is used to ensure that the variations in the pressure-gradient and average shear are $\mathcal{O}(1)$, whereas the variation in the pressure and rotational-transform are $\mathcal{O}(\mu)$. The rationale for imposing such variations is that it is the pressure-gradient and shear, rather than the pressure and rotational-transform, that directly influences ballooning stability. All physically relevant quantities are similarly varied. The variations are constrained by requiring that the system satisfy $\nabla p = \mathbf{J} \times \mathbf{B}$ and that the magnetic field strength be undisturbed to lowest order. In this manner, a self-consistent, nearby equilibrium may be constructed for each variation $(\delta p', \delta \iota')$. Full details of this approach in stellarator geometry are presented in Ref.[7, 2, 11]

To lowest order in the variations, the curvature of the magnetic field is unchanged. It is the local shear which is primarily affected by the profile variations, where $s \rightarrow s + s_p \delta p' + s_\iota \delta \iota'$ and s_p and s_ι are analytic functions of the equilibrium. For the ballooning equation, the variations $\delta p', \delta \iota'$ alter the ballooning coefficients. Analytic expressions for $P \rightarrow P + \delta P$ and $Q \rightarrow Q + \delta Q$ may be derived [11]. The terms δP and δQ depend only on the original equilibrium, the eigenvalue-eigenfunction pair (γ, ξ) and the quantities $\delta p', \delta \iota'$:

$$\delta P = \delta P_{p'} \delta p' + \delta P_{\iota'} \delta \iota' + \delta P_{p'^2} \delta p'^2 + \delta P_{p'\,\iota'} \delta p' \delta \iota' + \delta P_{\iota'^2} \delta \iota'^2, \tag{4}$$
$$\delta Q = \delta Q_{p'} \delta p' + \delta Q_{\,\iota'} \delta \iota' + \delta Q_{p'^2} \delta p'^2 + \delta Q_{p'\,\iota'} \delta p' \delta \iota' + \delta Q_{\,\iota'^2} \delta \iota'^2. \tag{5}$$

Note that $\delta p'$ and $\delta p'^2$ are both of order unity (similarly for $\delta \iota', \delta \iota'^2$). For given $\delta p', \delta \iota'$, after calculating the perturbed coefficients, the perturbed ballooning equation may be resolved numerically (exactly) and marginal stability diagrams constructed. This is the conventional method for generating marginal stability diagrams as functions of p' and ι'.

Rather than solve the perturbed ballooning equation numerically, further analytic progress may be made. An analytic expression for how the ballooning mode growth rate varies with pressure-gradient and shear can be derived [11]. The crucial observation is that ballooning stability is an eigenvalue problem. For small profile variations, the impact of pressure-gradient and averaged shear variations can be treated as a perturbed eigenvalue problem. An appropriate expression for the change in the eigenvalue $\delta\gamma$ is

$$\delta\gamma = \frac{\partial \gamma}{\partial p'} \delta p' + \frac{\partial \gamma}{\partial\, \iota'} \delta \iota' + \frac{\partial^2 \gamma}{\partial p'^2} \delta p'^2 + \frac{\partial^2 \gamma}{\partial p' \partial\, \iota'} \delta p' \delta \iota' + \frac{\partial^2 \gamma}{\partial\, \iota'^2} \delta \iota'^2 + \ldots, \tag{6}$$

The dots '...' here indicate that the third order terms $\delta p'^3, \delta p'^2 \delta \iota', \delta p' \delta \iota'^2, \delta \iota'^3$, the fourth order terms $\delta p'^4, \delta p'^3 \delta \iota', \delta p'^2 \delta \iota'^2, \delta p' \delta \iota'^3, \delta \iota'^4$, and all higher order terms, are present. For the expression to be useful, it is required that the magnitude of the higher order terms

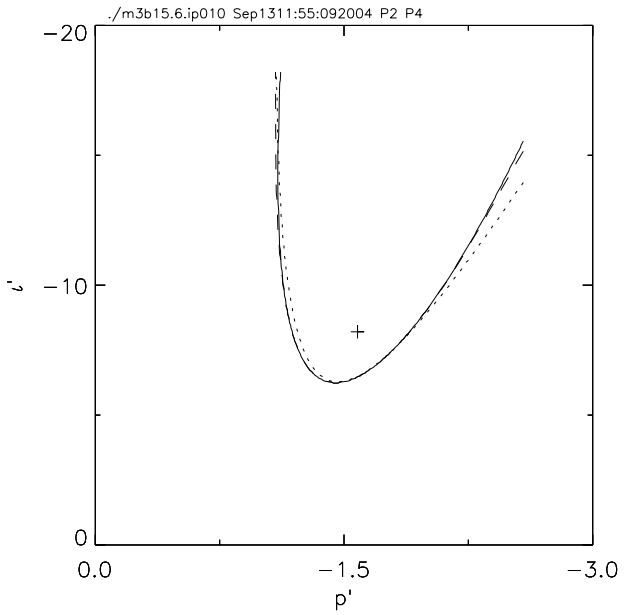

FIG. 1: Comparison of stability boundaries obtained from the exact eigenvalue solution (solid) with that obtained from Eqn.(6) using terms up to second order (dotted) and terms up to fourth order (dashed) for a quasi-poloidal hybrid stellarator.

rapidly diminish so that a truncated form of Eqn.(6) is meaningful. This paper will investigate the accuracy of various truncated forms of this expression.

Using the shorthand notation, $\langle\xi_1|F|\xi_2\rangle \int \xi R\, \xi d\eta = \int \xi_1 F \xi_2 d\eta$, the first order derivative $\partial\gamma/\partial p'$ is given by

$$\frac{\partial\gamma}{\partial p'} = \langle\xi|\partial_\eta \delta P_{p'} \partial_\eta + \delta Q_{p'} - \gamma \delta R_{p'}|\xi\rangle, \tag{7}$$

A similar expression holds for $\partial\gamma/\partial \iota'$. To calculate the second order derivatives, it is required to determine the first order variations, $\delta\xi_{p'}$ and $\delta\xi_{\iota'}$, in the eigenfunction, which are solved from

$$B\,\delta\xi_{p'} = \frac{\partial\gamma}{\partial p'} R\,\xi - \left[\partial_\eta \delta P_{p'} \partial_\eta + \delta Q_{p'} - \gamma \delta R_{p'}\right]\xi, \tag{8}$$

where $B = [\partial_\eta P \partial_\eta + Q - \gamma R]$ and a similar equation holds for $\delta\xi_{\iota'}$. The second order derivatives are then given by

$$\begin{aligned} \frac{\partial^2\gamma}{\partial p'^2} &= \langle\xi|\partial_\eta \delta P_{p'^2} \partial_\eta + \delta Q_{p'^2} - \gamma \delta R_{p'^2}|\xi\rangle + \langle\xi|\partial_\eta \delta P_{p'} \partial_\eta + \delta Q_{p'} - \gamma \delta R_{p'}|\delta\xi_{p'}\rangle \\ &- \frac{\partial\gamma}{\partial p'}\left(\langle\xi|R|\delta\xi_{p'}\rangle + \langle\xi|\delta R_{p'}|\xi\rangle\right), \end{aligned} \tag{9}$$

and similar expressions hold for $\partial^2\gamma/\partial p' \partial \iota'$ and $\partial^2\gamma/\partial \iota'^2$. The third, fourth and all higher order terms may be similarly calculated. All derivatives depend only on the initial equilibrium and the unperturbed eigenvalue–eigenfunction pair. Once they have been calculated, the influence of pressure-gradient and average shear variations on ballooning stability is known, and the marginal stability boundary, defined by $\gamma + \delta\gamma = 0$, may immediately be determined from Eqn.(6). Furthermore, noting that positive γ indicates

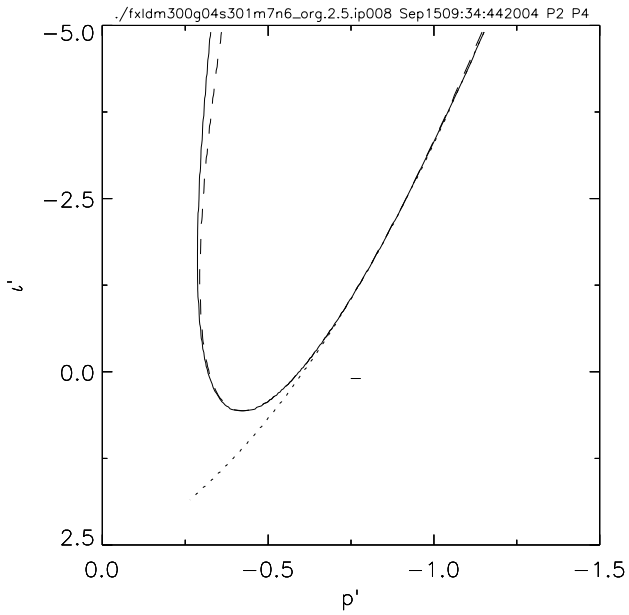

FIG. 2: Comparison of stability boundary obtained from the exact eigenvalue solution (solid) with that obtained from Eqn.(6) using terms up to second order (dotted) and terms up to fourth order (dashed) for an LHD-like configuration.

instability, and that increasing pressure-gradient corresponds to $\delta p' < 0$, we note that for a small increase $-\delta p'$, the eigenvalue γ will increase if $\partial\gamma/\partial p' < 0$ and decrease if $\partial\gamma/\partial p' > 0$. This result enables a criterion to determine, for a given configuration, if whether increased pressure-gradient will be stabilizing or destabilizing. Furthermore, a second stable region is indicated if $\partial^2\gamma/\partial p'^2 < 0$. This latter statement must be tempered by the additional requirement that the third and higher order terms in Eqn.(6) can safely be ignored. The following results will show that this is not always the case. In general, it is necessary to consider higher order terms. The following section will compare predictions of various truncated forms of Eqn.(6) with the exact result, as obtained be re-solving the perturbed ballooning eigenvalue equation numerically, for various stellarator configurations.

To consider realistic stellarator equilibria, we use the VMEC [13] code to compute an equilibrium. To solve the ballooning equation, we adopt a finite difference method, as described by Sanchez et al. [14]. The eigenfunction is represented by a discrete set of $(2N+1)$ points ξ_i equally spaced along a selected field line on the 'full-grid' according to $\eta_i = -\eta_\infty + (i-1)\Delta$, with the grid-spacing $\Delta = \eta_\infty/N$ chosen to give about 100 grid points along the field line per poloidal transit, with the boundary conditions $\xi_1 = \xi_{2N+1} = 0$, and where η_∞ is chosen sufficiently large to contain the mode (several poloidal transits). The equation to be solved becomes a set of $2N-1$ linear equations of the form

$$\frac{P_{i+\frac{1}{2}}}{\Delta}\frac{(\xi_{i+1}-\xi_i)}{\Delta} - \frac{P_{i-\frac{1}{2}}}{\Delta}\frac{(\xi_i-\xi_{i-1})}{\Delta} + Q_i\xi_i = \gamma R_i\xi_i.$$

Here, Q_i and R_i are calculated on the full-grid at η_i, whereas $P_{i+\frac{1}{2}}$ is calculated on the half-grid $\eta_i + \Delta/2$. This is a matrix equation, $M\xi = \gamma\xi$, where M is tri-diagonal. The largest eigenvalue and its eigenfunction are then solved using standard numerical routines [14]. The same finite difference approximation is suitable for calculating what amounts to be inner products appearing in the expressions for the derivatives.

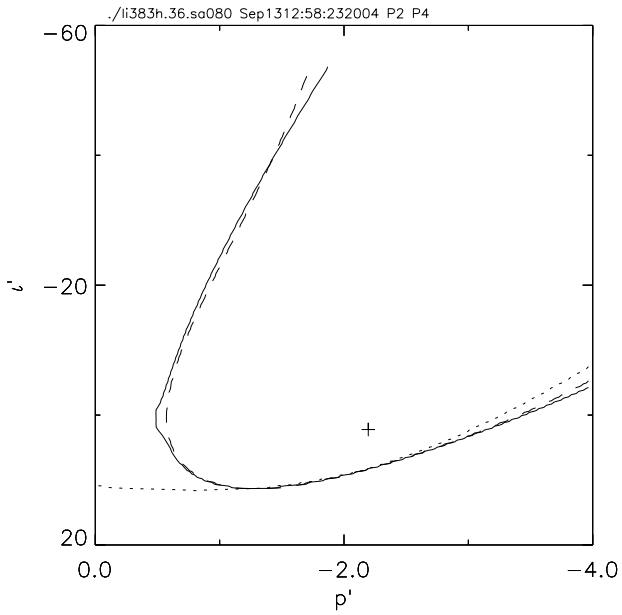

FIG. 3: Comparison of stability boundary obtained from the exact eigenvalue solution (solid) with that obtained from Eqn.(6) using terms up to second order (dotted) and terms up to fourth order (dashed) for an NCSX-like configuration.

3. Results.

Marginal stability diagrams for various configurations will now be presented. In all of the diagrams, the location of the original equilibrium surface in (p', ι') space is indicated with '+' if that field line is unstable or with '−' if that surface is stable. Also, only the symmetric field line passing through $\theta = 0, \zeta = 0$ has been considered, with the 'ballooning-angle' chosen $\eta_k = 0$. A comprehensive ballooning analysis of the equilibria considered here would consider all field lines, on all surfaces, with all values of the ballooning eigenvalue η_k. This is not attempted here; rather it is the intention of this article to illustrate the application of using perturbed eigenvalue analysis to predict the stability of the selected field line in the neighboring equilibria.

In Fig.(1) is shown the stability diagram for a for a three field period, quasi-poloidal stellarator-tokamak hybrid studied by Ware et al. [3]. The marginal stability curve obtained by re-solving the perturbed eigenvalue equation exactly at 200×200 points on the $(\delta p', \delta\iota')$ space is compared to the stability curve obtained from Eqn.(6) using terms up to and including second order (dotted) and up to and including fourth order (dashed). The quantitative agreement between the semi-analytic expression Eqn.(6) and the numerical value is very good, particularly considering the large variation in $(\delta p', \delta\iota') \sim (p', \iota')$. In this case, the truncated expression Eqn.(6) to second order provides a good estimate of the full stability boundary, and the fourth order expression is better still. Note that the dotted and dashed curve required only one eigenvalue-eigenfunction calculation, whereas the solid curve required 200×200.

In Fig.(2) is shown the corresponding stability diagram for an LHD-like configuration. For this case, the marginal stability boundary obtained by truncating Eqn.(6) at second order fails to reproduce the full boundary. In this case, it is necessary to go to higher order. The fourth order expression does give good agreement with the exact curve. This behavior is repeated in the stability boundary for an NCSX-like configuration Fig.(3).

4. Discussion.

As it is not a-priori known to what order the expression for the perturbed eigenvalue Eqn.(6) must be extended to obtain reliable results, a practical application of this theory would require higher order terms to be calculated until the magnitude of these extra terms becomes sufficiently small. Though the expressions for the higher order derivatives $\partial^{(n)}\gamma/\partial p'^{(n)}, \ldots$, do become quite lengthy, they are easily calculated numerically. Ultimately, all the derivatives depend only on the original equilibrium, and the derivatives (and perturbed eigenfunctions) of lower order.

If the expression Eqn.(6) truncated to second order was reliable, the second stability properties of the configuration would be described by $\partial\gamma/\partial p'$ and $\partial^2\gamma/\partial p'^2$. In this case, a second stable region will exist if $\partial^2\gamma/\partial p'^2 < 0$. This is the case for the quasi-poloidal configuration Fig.(1). This, however, is not generally the case, and for the LHD-like and the NCSX-like configurations, higher-order expressions must be employed.

It would be of interest to determine what property of the configuration determines at what order the expression can be truncated. In most applications of experimental interest, the magnitude of the variations $\delta p', \delta\iota'$ are likely to be small, and the smaller the $\delta p', \delta\iota'$ the more accurate truncated expressions will be.

The marginal stability diagrams are geometry dependent, and differing geometry can have a dramatic impact on ballooning stability. In particular, for a given configuration, the geometry of flux surfaces near the magnetic axis may be sufficiently different from those near the plasma edge. It may be the case that a configuration will have a strong second stable region near the plasma core, but a weaker second stable region near the plasma edge. This in fact is the case for the LHD-like configuration. Also, for large variations in the plasma pressure, the geometry of the configuration may change. The change in ballooning stability caused by pressure induced variations in the geometry is smaller than that caused by pressure induced variations in the local shear, but nevertheless if the geometry changes significantly it will be necessary to recompute the marginal stability diagram.

In stellarator equilibria, the ballooning eigenvalue is local to each field line. The eigenvalue also depends on the ballooning angle η_k. It is often the case in tokamak configurations that the first stable boundary is determined by $\eta_k = 0$, but that the second stable boundary is determined by non-zero η_k. A comprehensive ballooning analysis must consider all field lines for all values of η_k.

The eigenvalue perturbation theory is valid for discrete (non-degenerate) eigenvalues and as such the theory is valid only for the unstable spectrum (though discretization will eliminate the continuous spectrum). This problem may be avoided by adjusting the pressure-gradient using the method of profile variations to find an unstable eigenmode. The stability diagram may then be based on this point.

The analysis is completely general and applicable to axi-symmetric devices such as tokamaks, where it is known that shaped configurations possess stronger second-stable regions. The analysis presented in this letter may be of benefit to stellarator optimization routines and future stellarator designs, existing stellarator experiments, and also to the study of micro-instabilities which employs a similar eikonal approach.

[1] J.M. Greene and M.S. Chance. *Nucl. Fus.*, 21(4):453, 1981.

[2] S.R. Hudson and C.C. Hegna. *Phys. Plasmas*, 10(12):4716, 2003.

[3] A.S. Ware, S.P. Hirshman, D.A. Spong, et al. *Phys. Rev. Lett.*, 89(12):125003–1, 2002.

[4] S.R. Hudson, C.C. Hegna, R. Torasso, and A. Ware. *Plasma Phys. Controlled Fusion*, 46:869–876, 2004.

[5] C.C. Hegna and S.R. Hudson. *Phys. Rev. Lett.*, 87(3):035001–1, 2001.

[6] C.C. Hegna and S.R. Hudson. *Phys. Plasmas*, 9(5):2014, 2002.

[7] C.C. Hegna and N. Nakajima. *Phys. Plasmas*, 5(5):1336, 1998.

[8] J.H.Harris, M.Murakami, B.A.Carreras, et al. *Phys. Rev. Lett.*, 63(12):1249, 1989.

[9] B.A. Carreras, N. Dominguez, V.E. Lynch, et al, *Fusion Technol.*, 23:71, 1993.

[10] T. Matsumoto, Y. Nakamura, and M. Wakatani. *J. Phys. Soc. Jpn.*, 62(11):3904, 1993.

[11] S.R. Hudson and C.C. Hegna. *Phys. Plasmas*, 11(9):L53, 2004.

[12] A.H. Boozer. *Phys. Fluids*, 24(11):1999, 1981.

[13] S.P. Hirshman and O. Betancourt. *J.Comput. Phys.*, 96(1):99, 1991.

[14] R. Sanchez, S.P. Hirshman, J.C. Whitson, and A.S. Ware. *J.Comput. Phys.*, 161:576, 2000.